Elemental Redistribution and Interfacial Reaction Mechanism for the Flip Chip Sn-3.0Ag-(0.5 or 1.5)Cu Solder Bump with Al/Ni(V)/Cu Under-Bump Metallization During Aging

GUH-YAW JANG[1] and JENQ-GONG DUH[1,2]

1.—Department of Materials Science and Engineering National Tsing Hua University, Hsinchu, Taiwan, Republic of China. 2.—E-mail: jgd@mx.nthu.edu.tw

In flip chip technology, Al/Ni(V)/Cu under-bump metallization (UBM) is currently applicable for Pb-free solder, and Sn-Ag-Cu solder is a promising candidate to replace the conventional Sn-Pb solder. In this study, Sn-3.0Ag-(0.5 or 1.5)Cu solder bumps with Al/Ni(V)/Cu UBM after assembly and aging at 150°C were employed to investigate the elemental redistribution and reaction mechanism between solders and UBMs. During assembly, the Cu layer in the Sn-3.0Ag-0.5Cu joint was completely dissolved into solders, while Ni(V) layer was dissolved and reacted with solders to form $(Cu_{1-y},Ni_y)_6Sn_5$ intermetallic compound (IMC). The $(Cu_{1-y},Ni_y)_6Sn_5$ IMC gradually grew with the rate constant of 4.63×10^{-8} cm/sec$^{0.5}$ before 500 h aging had passed. After 500 h aging, the $(Cu_{1-y},Ni_y)_6Sn_5$ IMC dissolved with aging time. In contrast, for the Sn-3.0Ag-1.5Cu joint, only fractions of Cu layer were dissolved during assembly, and the remaining Cu layer reacted with solders to form Cu_6Sn_5 IMC. It was revealed that Ni in the Ni(V) layer was incorporated into the Cu_6Sn_5 IMC through slow solid-state diffusion, with most of the Ni(V) layer preserved. During the period of 2,000 h aging, the growth rate constant of $(Cu_{1-y},Ni_y)_6Sn_5$ IMC was down to 1.74×10^{-8} cm/sec$^{0.5}$ in the Sn-3.0Ag-1.5Cu joints. On the basis of metallurgical interaction, IMC morphology evolution, growth behavior of IMC, and Sn-Ag-Cu ternary isotherm, the interfacial reaction mechanism between Sn-3.0Ag-(0.5 or 1.5)Cu solder bump and Al/Ni(V)/Cu UBM was discussed and proposed.

Key words: Flip chip, intermetallic compound, Sn-Ag-Cu solder, interfacial reaction, growth kinetics, Al/Ni(V)/Cu UBM

INTRODUCTION

Flip chip technology, explored since the 1960s, possesses several advantages, such as high input/output connects, low cost, high-frequency performance, and easy assembly.[1] It has thus become one of the most attractive processing methods in microelectronics.[2–4] In this technology, multilayered thin film metallization is used for under-bump metallization (UBM) as bonding pad on Si chips. The thin film UBM is crucial due to its low residual stress, diminishing risk in Si cratering around the metallization.[5] Al/Ni(V)/Cu UBM is currently introduced in the flip chip technology when Sn-Ag-Cu solder is employed.[5–8] In this UBM, Cu acts as a wetting layer to the solder and Ni(V) as an efficient barrier layer to the diffusion of solder.

The interfacial reactions between Sn-Ag-Cu solder and Al/Ni(V)/Cu UBM after multiple reflows and aging testing have been reported recently.[5–9] Zhang et al.[8] reported that $(Cu,Ni)_6Sn_5$ IMC formed between Sn-3.5Ag-1Cu solder and Al/Ni(V)/Cu UBM during ten reflows at 260°C. It was revealed that the Ni(V) layer was gradually replaced by the Sn patches with reflows. In Sn-37Pb solder bump reflowed at 220°C, $(Cu,Ni)_6Sn_5$ IMC also formed at the interface of solders and UBMs. However, Ni(V) remained nearly intact even up to 20 reflows. Tu et al. claimed that the different interfacial reaction was due to the difference of Cu solubility in Sn-Ag-Cu and Sn-Pb system.[5] Tu et al. further investigated the effect of Cu content on the interfacial reaction between bulk Sn-Cu solders and Al/Ni/Cu thin-film metallizations.[10]

(Received March 9, 2006; accepted May 8, 2006)

After one reflow at 240°C, the Ni layer of Al/Ni/Cu was almost consumed by Sn-0.7Cu. On the other hand, most of Ni layer was preserved with Sn-3Cu even after ten reflows.

Recently, the metallurgical reaction in the Sn-3.0Ag-(0.5 or 1.5)Cu solder bump with Al/Ni(V)/Cu UBM was reported.[9] Nevertheless, literature on mechanisms of interfacial reaction and compound formation at the solder/UBM interface is limited and not well understood. The aim of this study is to establish the mechanism of interfacial reaction between Sn-3.0Ag-(0.5 or 1.5)Cu solder bump and Al/Ni(V)/Cu UBM through the investigation of detailed metallurgical reaction, IMC morphology evolution, and growth behavior of IMC. In addition, the influence of Sn patches on the IMC growth is also discussed.

EXPERIMENTAL PROCEDURES

The schematic diagram of the flip chip Sn-3.0Ag-(0.5 or 1.5)Cu solder joints used in this study is shown in Fig. 1. The test chip with ball-shaped Sn-3.0Ag-(0.5 or 1.5)Cu solder bumps was flipped over and assembled to a bismaleimide triazine (BT) substrate with Sn-3.0Ag-0.5Cu presolder bumps. The interconnection line on the Si chip was sputtered Cu of 1 μm. Then 1.2 μm Al was sputtered on the Cu conductor. A trilayer of Al/Ni(V)/Cu thin film was further sputtered on the metallized substrate to form an UBM structure. The thicknesses of Al, Ni(V), and Cu were 1.2 μm, 1.0 μm, and 0.5 μm, respectively. After the UBM was deposited onto the Si wafer, the Sn-3.0Ag-(0.5 or 1.5)Cu solder paste was stencil printed on the Al/Ni(V)/Cu UBM and then reflowed at 240°C. The diameter of flip chip solder bump was 100 μm. On the BT substrate, Sn-3.0Ag-0.5Cu solder paste was stencil printed on the electroless Ni-P (EN)/immersion Au finished bonding pads, followed by the reflow at 240°C. The thicknesses of electroless Ni-P and immersion Au were about 5 μm and 0.1 μm, respectively, and the diameter of bonding pad on the BT substrate was 90 μm. After assembly, the gaps between the Si chip and the BT substrate were filled with underfills.

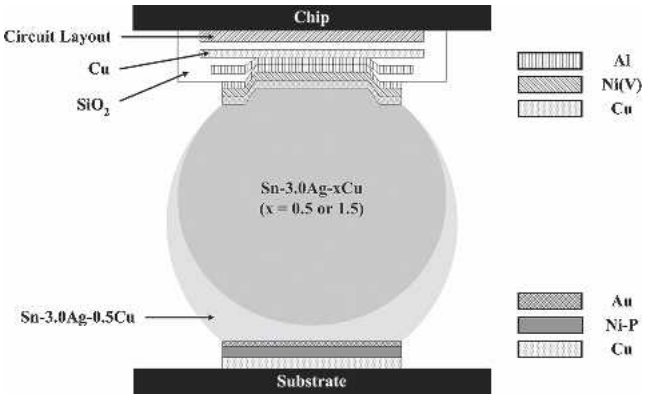

Fig. 1. Schematic illustration of the flip chip Sn-3.0Ag-(0.5 or 1.5)Cu solder joint employed in this study. The test chip with ball-shaped Sn-3.0Ag-(0.5 or 1.5)Cu solder bumps was flipped over and assembled to a BT substrate with Sn-3.0Ag-0.5Cu presolder bumps. A sputtered trilayer of 1.2 μm Al/1.0 μm Ni(V)/0.5 μm Cu thin film was used as UBM structure on the chip. In addition, the surface finish on the Cu pad at BT substrate was the electroless Ni-P(5μm)/immersion Au(0.1μm) structure.

The as-assembled samples were aged at 150°C for 168 h, 500 h, 1,000 h, 1,500 h, and 2,000 h, respectively. The as-assembled and aged samples were first cold-mounted in epoxy and then sectioned by a slow-speed diamond saw. The cross-sectional samples were ground, polished, and etched with one part hydrochloric acid, nine parts methanol at room temperature for interfacial microstructural analysis. To reveal the morphologies of interfacial products, the solder bumps were etched directly with one part nitric acid, one part acetic acid, and four parts glycerin at 80°C. The morphologies of interfacial products between solder bumps and UBMs were analyzed with a field-emission scanning electron microscope (FE-SEM; JSM-6500F, JEOL, Japan; Electron Optics Laboratory, Tokyo, Japan). The compositions of phases in the solder joints were quantitatively measured with a conventional electron probe microanalyzer (EPMA; JXA-8800M, JEOL) with the aid of a ZAF program,[11] as well as a recently developed field-emission EPMA (FE-EPMA 8500F, JEOL).

RESULTS AND DISCUSSION

Elemental Redistribution and Composition of IMC Due to Metallurgical Reaction Between Sn-3.0Ag-0.5Cu Solder Bump and Al/Ni(V)/Cu UBM During Aging

Figure 2a exhibits the interfacial morphology between solder bumps and UBMs in the as-assembled Sn-3.0Ag-0.5Cu joint. Only one interfacial product was found between the solder and the Ni(V) layer after assembly. Before microstructure study by EPMA, it should be noted that the activation volume due to the interaction between the electron beam in EPMA and the tested joint should be smaller than the size of the interfacial product under investigation.[11] To achieve a reliable quantitative result, a preliminary task was carried out to select the appropriate accelerating voltage and beam current.[12,13] The average composition of the interfacial product after at least ten measurements was 45.9 at.% Sn-36.6 at.% Cu-17.5 at.% Ni. The ratio of the atomic percentage of (Cu + Ni) to Sn was (36.6 + 17.5):(45.9), which is close to 6:5. As a result, this interfacial product was thus identified as $(Cu_{1-y},Ni_y)_6Sn_5$ IMC.

The Cu layer was completely consumed, and white patches were observed in the Ni(V) layer after as-assembly, as shown in Fig. 2a. In fact, the white patches were also observed between Sn-3.5Ag-1.0Cu and Al/Ni(V)/Cu UBM after 5 reflows in Tu's study,[5] in which the white patches were denoted as Sn patches. By x-ray color mapping in FE-EPMA, the Sn patch was identified as Sn-rich phase with small

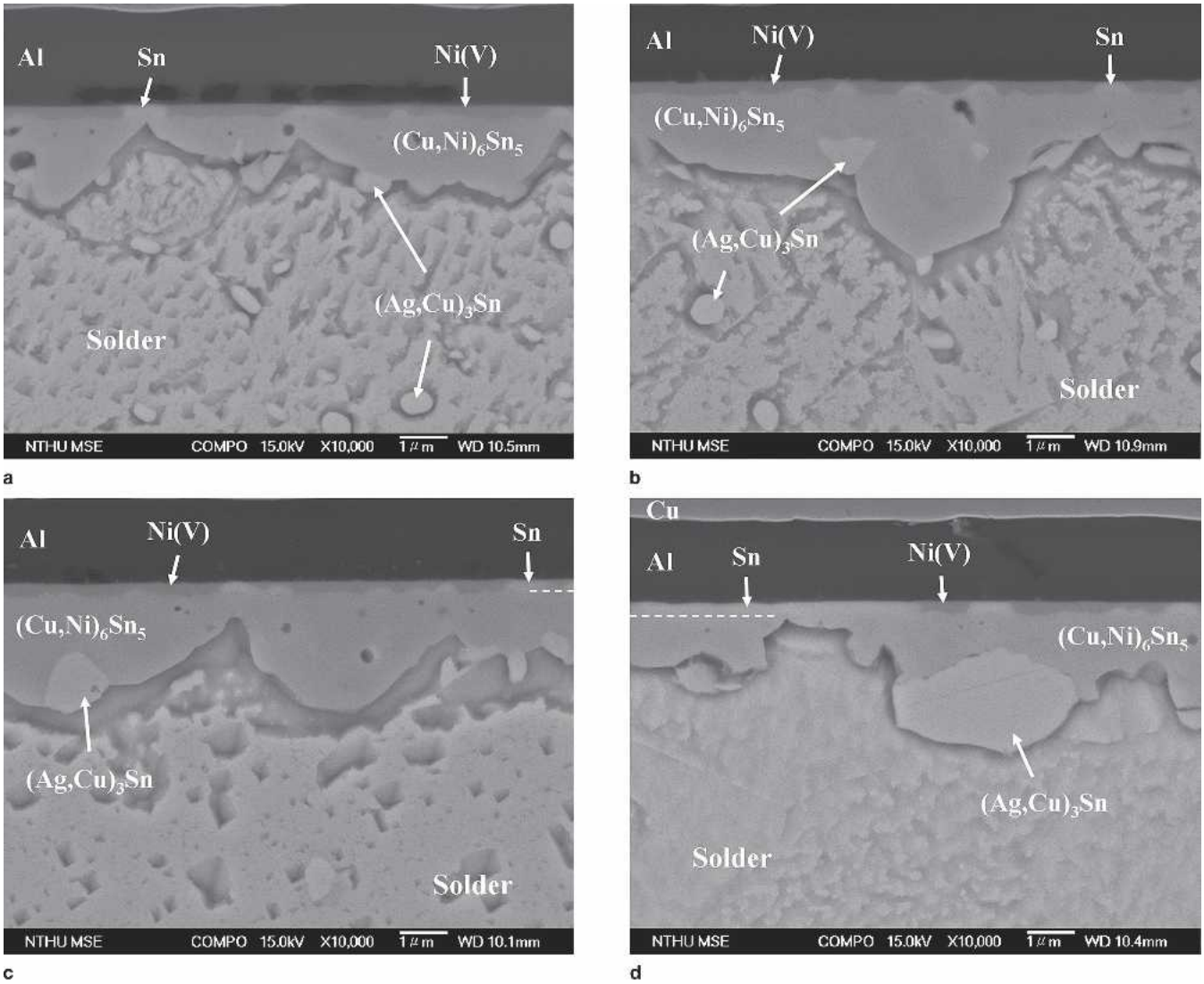

Fig. 2. Cross-sectional image of interfacial morphology at chip side in the Sn-3.0Ag-0.5Cu joints after (a) assembly and aging at 150°C for various time, (b) 500 h, (c) 1,000 h, and (d) 2,000 h.

amounts of Cu, Ni, and V, as indicated in Fig. 3. In addition, there was another phase, which was adjacent to the $(Cu_{1-y},Ni_y)_6Sn_5$ IMC, in lighter contrast observed in the solder (Figs. 2a and 3). After detailed quantitative analysis by FE-EPMA, the composition of this white product was 25.0 ± 0.8 at.% Sn-74.2 ± 0.7 at.% Ag-0.8 ± 0.1 at.% Cu, in which the ratio of (Ag + Cu) to Sn approached 3:1. The white product was thus considered as Ag_3Sn with dissolved Cu. According to Hume-Rothery rule, some Ag in Ag_3Sn was substituted by Cu to form $(Ag_{1-z},Cu_z)Sn$ IMC.[9,14,15]

The as-assembled Sn-3.0Ag-(0.5 or 1.5)Cu joints were aged at 150°C for 168 h, 500 h, 1,000 h, 1,500 h, and 2,000 h, respectively. Typical interfacial morphologies between solder bumps and UBMs after various aging time are presented in Figs. 2b–2d. During aging for 2,000 h, only $(Cu_{1-y},Ni_y)_6Sn_5$ IMC formed at the interface, as shown in Figs. 2b–2d. The composition of $(Cu_{1-y},Ni_y)_6Sn_5$ IMC at the chip side was evaluated by EPMA and is listed in Table I. It was revealed that the Ni(V) layer was gradually consumed with aging time. On the other hand, the amount of Sn patches increased with aging time. The average thickness fractions of Sn patches to [Ni(V) layer + Sn patches] after 168 h, 500 h, 1,000 h, 1,500 h, and 2,000 h aging were 18.6%, 21.8%, 24.1%, 32.0%, and 61.6%, respectively. The dependence of Sn patch fractions with respect to the aging time is presented in Fig. 4.

To further investigate the morphology of the $(Cu_{1-y},Ni_y)_6Sn_5$ IMC, an etching solution was introduced to remove the bulk solder. Figure 5 shows the top-view micrographs of $(Cu_{1-y},Ni_y)_6Sn_5$ in the Sn-3.0Ag-0.5Cu joints after assembly and aging. The $(Cu_{1-y},Ni_y)_6Sn_5$ IMC appeared rod-like. The top-view morphology in Fig. 5 as well as the cross-sectional images shown in Fig. 2 demonstrated that the $(Cu_{1-y},Ni_y)_6Sn_5$ IMC gradually grew until 500 h aging. However, after aging for more than 500h, $(Cu_{1-y},Ni_y)_6Sn_5$ IMC was dissolved slowly with aging time.

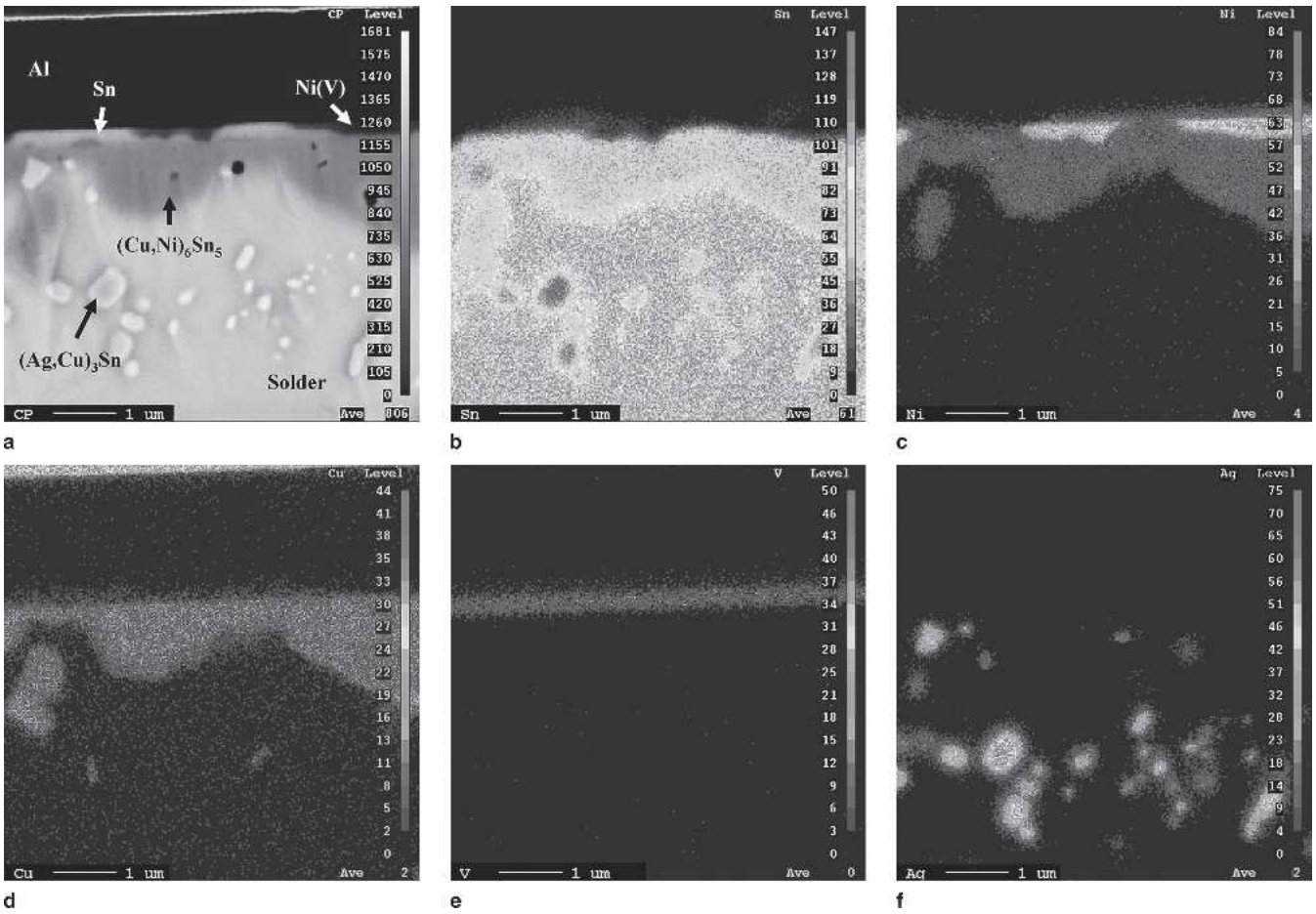

Fig. 3. Interface between the Sn-3.0Ag-0.5Cu solder and Al/Ni(V)/Cu UBM after as-assembly: (a) backscattered electron imaging and x-ray color mapping of (b) Sn, (c) Ni, (d) Cu, (e) V, and (f) Ag.

Table I. Measured y values in $(Cu_{1-y}, Ni_y)_6Sn_5$ IMCs formed at the chip side in the Sn-3.0Ag-(0.5 or 1.5)Cu joints aged at 150°C.

	Aging time (h)				
Solder joint	**0**	**168**	**500**	**1000**	**1500**
Sn-3.0Ag-0.5Cu	0.29–0.32	0.21–0.32	0.21–0.32	0.15–0.32	0.11–0.32
Sn-3.0Ag-1.5Cu	0.05–0.11	0.04–0.11	0.04–0.11	0.03–0.11	0.03–0.11

Composition Variation in IMC and Metallurgical Reaction Between Sn-3.0Ag-1.5Cu Solder Bump and Al/Ni(V)/Cu UBM During Aging

In the as-assembled Sn-3.0Ag-1.5Cu joint, there is also only one interfacial product formed near the chip side (Fig. 6a). After quantitative analysis of EPMA, the interfacial product was also identified as the $(Cu_{1-y},Ni_y)_6Sn_5$ IMC. However, the concentration of dissolved Ni in $(Cu_{1-y},Ni_y)_6Sn_5$ in the as-assembled Sn-3.0Ag-1.5Cu joint was less than that in the as-assembled Sn-3.0Ag-0.5Cu joint, as shown in Table I.

During aging at 150°C, the $(Cu_{1-y},Ni_y)_6Sn_5$ IMC formed between the solder and the Ni(V) layer (Figs. 6b–6d). The content of dissolved Ni in the $(Cu_{1-y},Ni_y)_6Sn_5$ in the Sn-3.0Ag-1.5Cu joints was still smaller than that in the Sn-3.0Ag-0.5Cu joints even up to 1,500 h aging (Table I). In both Sn-3.0Ag-0.5Cu and Sn-3.0Ag-1.5Cu joints, Ni atom diffused from the Ni(V) layer into $(Cu_{1-y},Ni_y)_6Sn_5$ IMC during aging, and thus the Ni content in $(Cu_{1-y},Ni_y)_6Sn_5$ IMC gradually decreased when approaching the solder. The composition variation of $(Cu_{1-y},Ni_y)_6Sn_5$ IMC in the 500 h aged Sn-3.0Ag-1.5Cu joints was typically demonstrated. The Ni content in $(Cu_{1-y},Ni_y)_6Sn_5$ decreased from 6.1 at.% (y = 0.11) at the $(Cu_{1-y},Ni_y)_6Sn_5$/ UBM interface to 2.2 at.% (y = 0.03) at the solder/$(Cu_{1-y},Ni_y)_6Sn_5$ interface. The variations of compositions in $(Cu_{1-y},Ni_y)_6Sn_5$ IMC for both Sn-3.0Ag-0.5Cu and Sn-3.0Ag-1.5Cu joints during aging are listed in Table I. It was interesting to point out that the Ni(V) layer was preserved even after 2,000 h aging, and no Sn patches formed between solders and UBMs even up to 2,000 h aging.

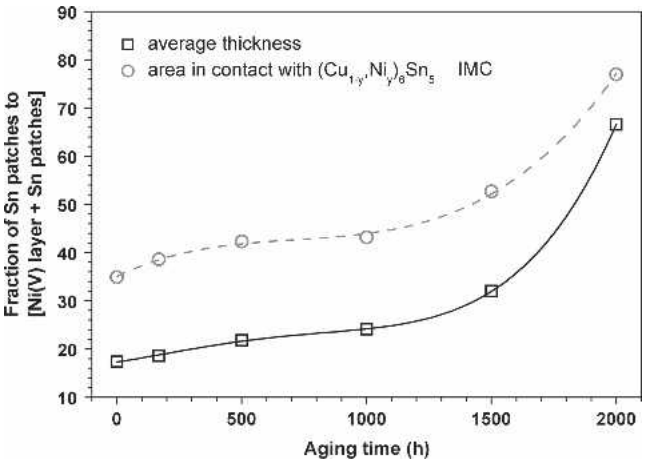

Fig. 4. Fractions of Sn patches to [Ni(V) layer + Sn patches] for the average thickness and the area in contact with $(Cu_{1-y},Ni_y)_6Sn_5$ IMC in the Sn-3.0Ag-0.5Cu joints during aging at 150°C.

The top-view micrographs of the $(Cu_{1-y},Ni_y)_6Sn_5$ IMC in the Sn-3.0Ag-1.5Cu joints after as-assembly and aging are illustrated in Fig. 7. The morphology of the $(Cu_{1-y},Ni_y)_6Sn_5$ for Sn-3.0Ag-1.5Cu joints was nodular-type and dissimilar to that formed in the Sn-3.0Ag-0.5Cu joints. Statistically, the grain-size distributions of the $(Cu_{1-y},Ni_y)_6Sn_5$ IMCs in the Sn-3.0Ag-1.5Cu joints after assembly and 168 h, 1,000 h, and 2,000 h aging were 0.8–2.0 μm, 1.2–4.0 μm, 1.4–5.3 μm, and 1.7–7.8 μm, respectively. It was evident from both the cross-sectional image in Fig. 6 and the top-view morphology in Fig. 7 that the $(Cu_{1-y},Ni_y)_6Sn_5$ IMCs in the Sn-3.0Ag-1.5Cu joints gradually grew with aging time.

IMC Growth Kinetics During Aging Treatment

The thickness of $(Cu_{1-y},Ni_y)_6Sn_5$ IMC was measured at specific aging condition to investigate

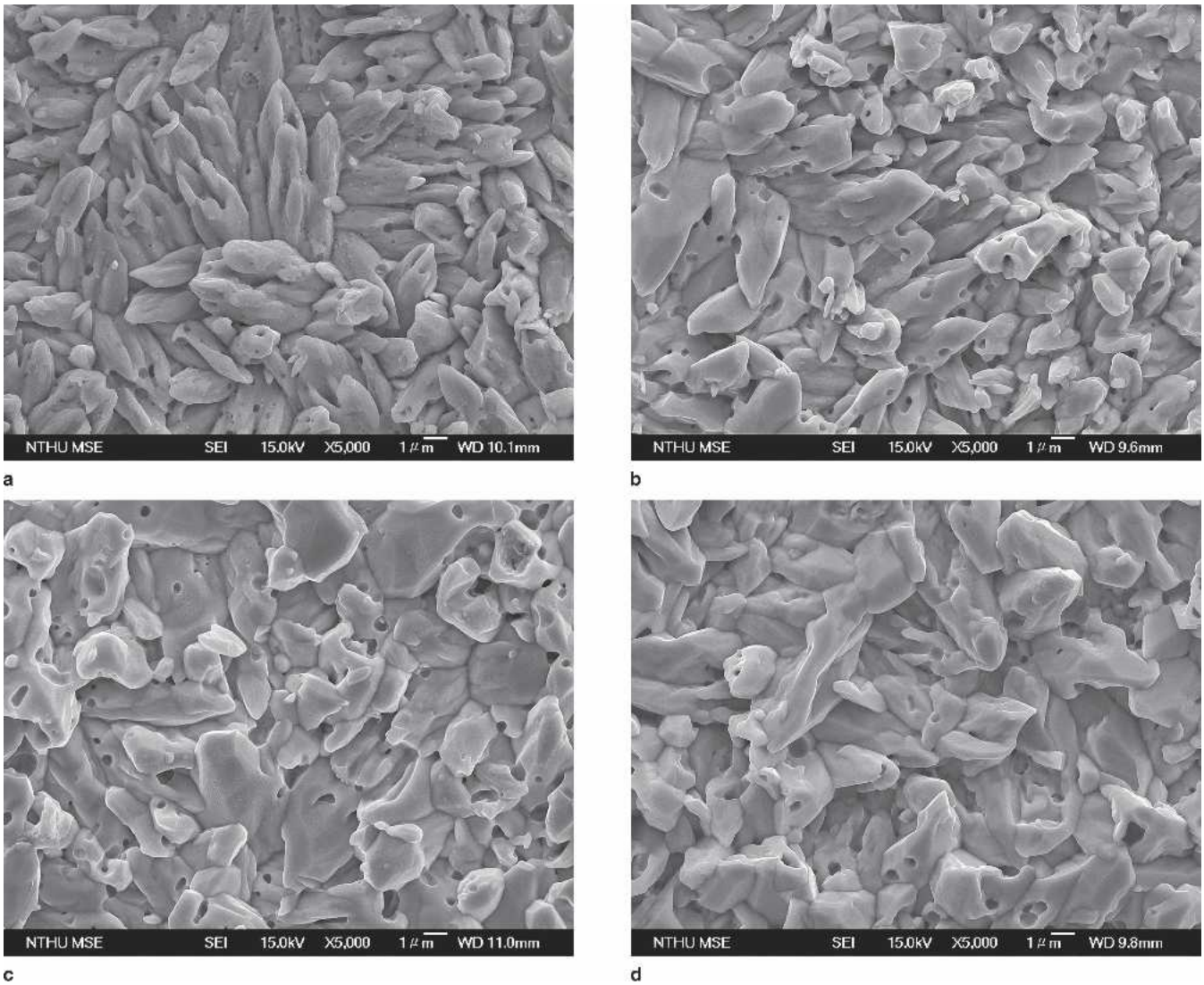

Fig. 5. Top view morphology of $(Cu,Ni)_6Sn_5$ IMC at chip side in the Sn-3.0Ag-0.5Cu joints after (a) assembly and aging at 150°C for (b) 168 h, (c) 1,000 h, and (d) 2,000 h.

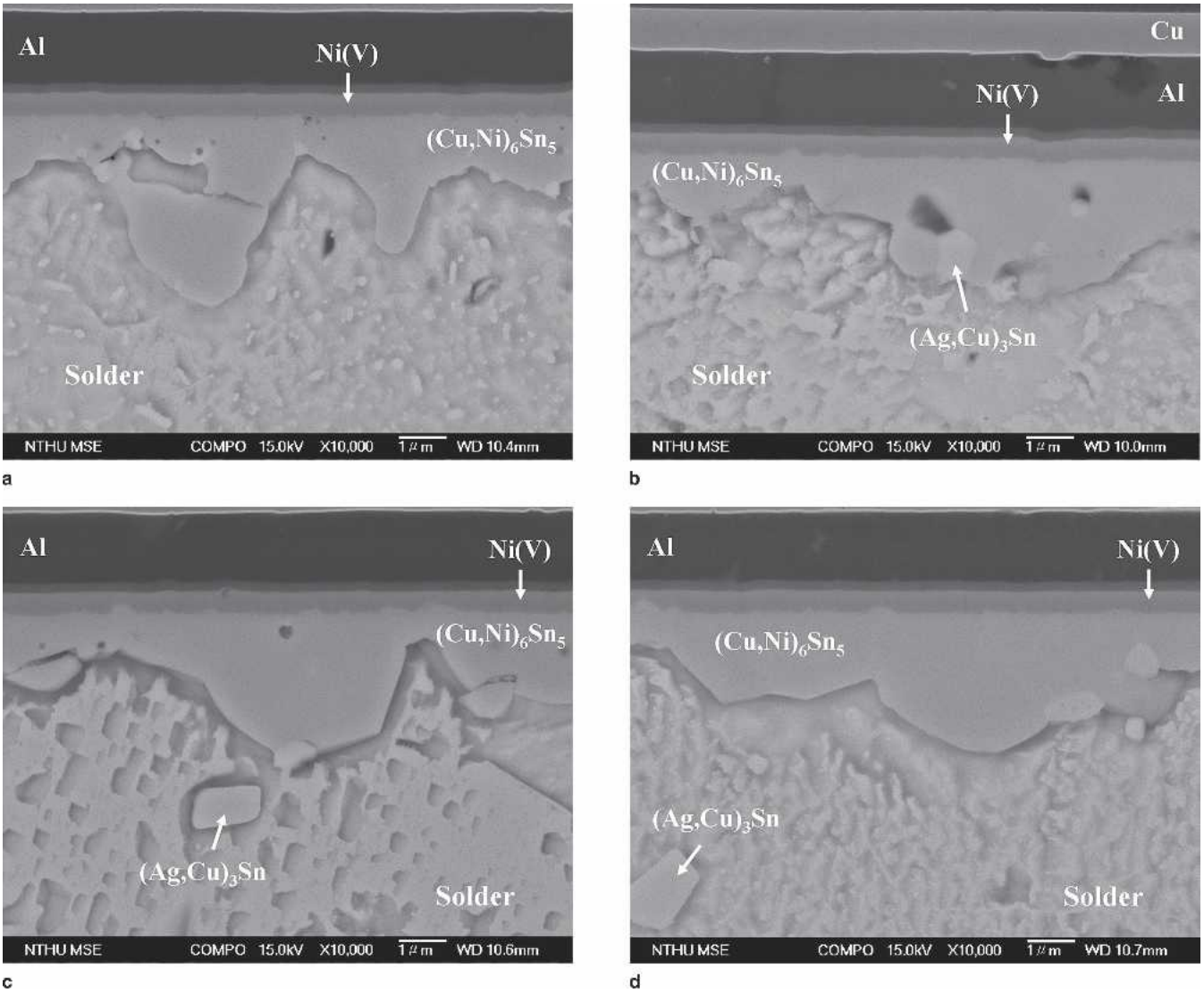

Fig. 6. Cross-sectional image of interfacial morphology at chip side in the Sn-3.0Ag-1.5Cu joints after (a) assembly and aging at 150°C for various time (b) 500 h, (c) 1,000 h, and (d) 2,000 h.

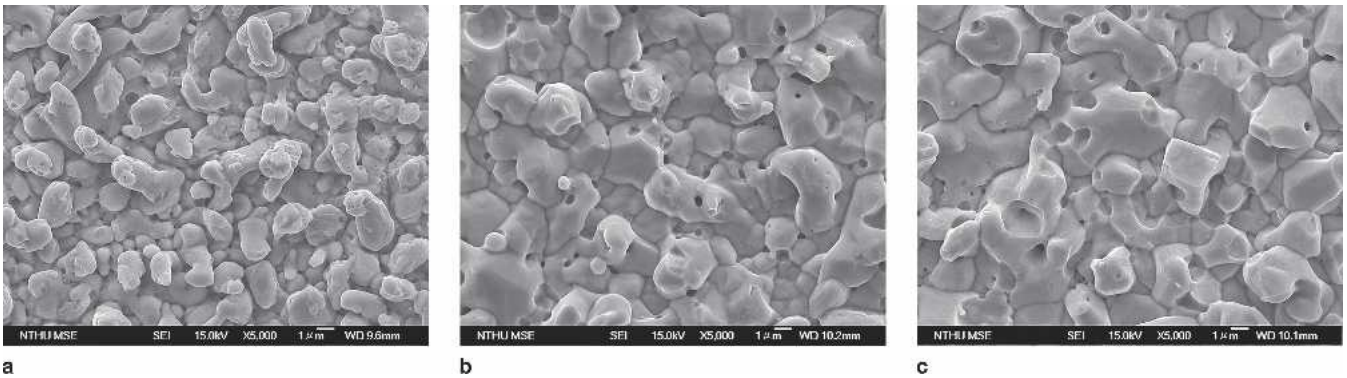

Fig. 7. Top-view morphology of $(Cu,Ni)_6Sn_5$ IMC at chip side in the Sn-3.0Ag-1.5Cu joints after (a) assembly and aging at 150°C for (b) 1,000 h and (c) 2,000 h.

the kinetics of $(Cu_{1-y},Ni_y)_6Sn_5$ growth. In general, the growth rate of an intermediate phase during the interdiffusion of metals with volume diffusion predominated follows the parabolic rate law:[16–21]

$$x - x_0 = kt^{1/2} \quad (1)$$

where x is the thickness of intermediate phase layer, x_0 represents the initial thickness of

intermediate phase layer, k indicates the rate constant dependent upon the interdiffusion coefficients, and t is the aging time.

The thickness of $(Cu_{1-y},Ni_y)_6Sn_5$ IMC vs. square root of aging time is shown in Fig. 8. In the Sn-3.0Ag-0.5Cu joints, the growth behavior of $(Cu_{1-y},Ni_y)_6Sn_5$ before 500 h aging was different with that after more than 500 h aging. This was in agreement with the observation from the top-view micrograph of $(Cu_{1-y},Ni_y)_6Sn_5$ IMC (Fig. 5). In general, the growth behavior of intermediate phase should follow the parabolic rate law during solid-state reaction.[16–21] However, an intermediate phase can be reacted back to one of its parent phases due to the supply limitation, which primarily acted as source for the growth of the phase.[22–24]

In the Sn-3.0Ag-0.5Cu joints, the Ni(V) layer and solders were regarded as the source for the growth of $(Cu_{1-y},Ni_y)_6Sn_5$ IMC during aging. Nevertheless, the Ni(V) layer was gradually replaced by Sn patches with aging time, as discussed previously. Thus, the formation of Sn patches played an important role in the growth of $(Cu_{1-y},Ni_y)_6Sn_5$ IMC. The average thickness fractions of Sn patches to [Ni(V) layer + Sn patches] after as-assembly and aging for 168 h, 500 h, 1,000 h, 1,500 h, and 2,000 h aging were 17.4%, 18.6%, 21.8%, 24.1%, 32.0%, and 61.6%, respectively. The Sn patch was scalloped-type or trapezoid-like, as shown in Figs. 2 and 3. Therefore, the contact area between Sn patches and $(Cu_{1-y},Ni_y)_6Sn_5$ IMC should be considered regarding the growth behavior of $(Cu_{1-y},Ni_y)_6Sn_5$. With the aid of cross-sectional images, the fractions of the area in contact with $(Cu_{1-y},Ni_y)_6Sn_5$ IMC for Sn patches to [Ni(V) layer + Sn patches] can be estimated to be 34.9%, 38.6%, 42.3%, 43.2%, 52.7%, and 77.0% after 0 h, 168 h, 500 h, 1,000 h, 1,500 h, and 2,000 h aging, as presented in Fig. 4. For aging longer than 500 h, the fractions of the area in contact with $(Cu_{1-y},Ni_y)_6Sn_5$ IMC for Ni(V) layer to [Ni(V) layer + Sn patches] were less than 57.7%. It was evident that the growth rate of $(Cu_{1-y},Ni_y)_6Sn_5$ IMC was smaller than the consumption rate after more than 500 h aging. Therefore, the growth kinetics for $(Cu_{1-y},Ni_y)_6Sn_5$ IMC in the Sn-3.0Ag-0.5Cu joints could be divided into two stages. Before 500 h aging, $(Cu_{1-y},Ni_y)_6Sn_5$ grew with a rate constant of 4.63×10^{-8} cm/sec$^{0.5}$. However, after 500 h aging, the $(Cu_{1-y},Ni_y)_6Sn_5$ IMC was dissolved, and the rate constant decreased to 2.60×10^{-8} cm/sec$^{0.5}$.

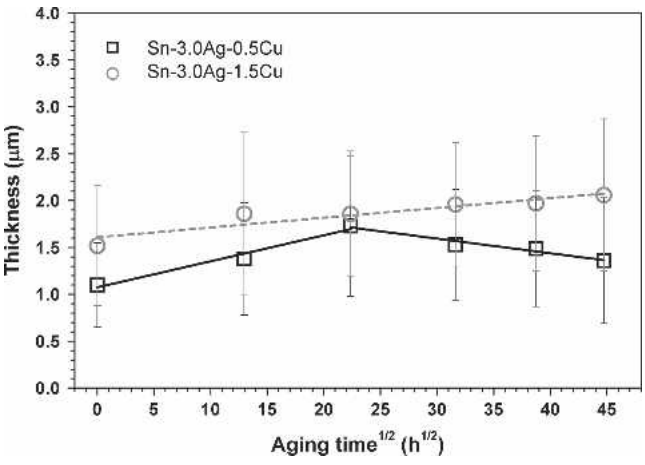

Fig. 8. Thickness of $(Cu_{1-y},Ni_y)_6Sn_5$ IMC formed in the Sn-3.0Ag-(0.5 or 1.5)Cu joints vs. square root of aging time at 150°C.

In the Sn-3.0Ag-1.5Cu joints, the Ni(V) layer was still retained even after 2,000 h aging. Moreover, no Sn patches formed at the interface of solder and UBM even up to 2,000 h aging. Thus, the growth behavior of $(Cu_{1-y},Ni_y)_6Sn_5$ IMC in the Sn-3.0Ag-1.5Cu joints followed the parabolic rate law during aging, as shown in Fig. 8. The growth rate constant of $(Cu_{1-y},Ni_y)_6Sn_5$ IMC in Sn-3.0Ag-1.5Cu joints as derived by Eq. (1) was 1.74×10^{-8} cm/sec$^{0.5}$ during 2,000 h aging.

In the study of Yu et al.,[20] both Cu_6Sn_5 and Cu_3Sn formed between the solder and the Cu substrate in the Sn-3.5Ag/Cu diffusion couples after aging at 70°C, 125°C, and 170°C for up to 1,000 h. The growth rate constants of overall IMCs, including Cu_6Sn_5 and Cu_3Sn, at 70°C, 125°C, and 170°C were 3×10^{-8}, 1.04×10^{-7}, and 5.92×10^{-7} cm/sec$^{0.5}$, respectively. Rizvi et al. reported that the growth rate constant for overall IMCs (Cu_6Sn_5 + Cu_3Sn) was 4.7×10^{-7} cm/sec$^{0.5}$ in the Sn-2.8Ag-0.5Cu/Cu diffusion couples after aging at 150°C.[21] However, the major IMC at the interface was Cu_6Sn_5. Thus, the growth rate constant for Cu_6Sn_5 should be close to that for overall IMCs in the Sn-2.8Ag-0.5Cu/Cu diffusion couples. Choi et al. further investigated the growth kinetics of Cu_6Sn_5 and Cu_3Sn IMCs in Sn-3.5Ag/Cu solder joints aged at various temperatures for long time periods up to 1400 h.[19] The growth rate constant of Cu_6Sn_5 IMC in the Sn-3.5Ag/Cu joints aged at 70°C, 100°C, 120°C, 150°C, and 180°C were 2.76×10^{-8} cm/sec$^{0.5}$, 2.92×10^{-8} cm/sec$^{0.5}$, 3.65×10^{-8} cm/sec$^{0.5}$, 1.41×10^{-7} cm/sec$^{0.5}$, and 4.63×10^{-7} cm/sec$^{0.5}$, respectively.

In comparison with literature data, the growth rate constant of IMC for the Sn-3.0Ag-(0.5 or 1.5)Cu joints with Al/Ni(V)/Cu UBM in this study was one order less than that in both Sn-Ag and Sn-Ag-Cu solder systems with Cu substrate.[19–21] In the literature, solders continually reacted with Cu substrate to form Cu_6Sn_5 and Cu_3Sn IMCs in the Sn-Ag based solder joints during aging. However, for Al/Ni(V)/Cu thin film UBM in this study, Cu thin film was reacted with Sn-Ag-Cu solder to form $(Cu_{1-y},Ni_y)_6Sn_5$ IMC, and it was rapidly exhausted in the assembly process. During aging, Ni in Ni(V) thin film was consumed and reacted with solders and then resulted in the growth of $(Cu_{1-y},Ni_y)_6Sn_5$ IMC if the Ni supply from the Ni(V) film was sufficient. Tu and Zeng reported that the reaction rate of Ni in the eutectic Sn-Pb solder diffusion couples was much slower in contrast to Cu substrate.[25] Similarly, the reaction rate of Ni(V) thin film should be smaller than that of Cu substrate. Consequently, the IMC growth rate in the

Sn-3.0Ag-(0.5 or 1.5)Cu joints with Al/Ni(V)/Cu UBM in this study was smaller than that in Sn-Ag based solder systems with Cu substrate in literatures.

Mechanism of Interfacial Reaction Between Solder Bump and UBM During Assembly and Aging Treatment

Recently, Tu et al. reported that the Ni(V) layer in the Al/Ni/Cu UBM was well protected even up to 20 reflow cycles in the Sn-37Pb solder bump.[5] For Sn-3.5Ag-1.0Cu solder bump, the Ni(V) layer disappeared and a layer of Sn separated the $(Cu_{1-y},Ni_y)_6Sn_5$ IMC from the Al layer after 20 reflow cycles. The different interfacial reactions between Sn-Pb and Sn-Ag-Cu systems could be related to the solubility of Cu in the molten solder. In the Sn-3.0Ag-(0.5 or 1.5)Cu flip chip solder bump with Al/Ni(V)/Cu UBM, the effect of Cu content in solder on the $(Cu_{1-y},Ni_y)_6Sn_5$ IMC formation was investigated.[9] If the entire Cu layer in the UBM dissolved into the Sn-Ag-Cu solder during assembly, the Cu concentration in the molten solder can be calculated as

$$C^{Cu}_{solder} = \frac{W^{Cu}_{solder\ bump} + W^{Cu}_{pre\text{-}solder} + W_{Cu\ layer}}{W_{solder\ bump} + W_{pre\text{-}solder} + W_{Cu\ layer}} \times 100\% \quad (2)$$

where W_I represents the weight of I, W^{Cu}_I is the weight of Cu in I. The detailed calculation for the Cu concentration in the molten solder was described elsewhere.[9] During assembly, the maximum Cu content in solder was estimated to be 0.98 wt.% for the Sn-3.0Ag-0.5Cu joint and 1.71 wt.% for the Sn-3.0Ag-1.5Cu joint.

On the basis of thermodynamic data in the Sn-Ag-Cu system,[5,26–30] an enlarged Sn corner of the Sn-Ag-Cu ternary isotherm at 240°C was proposed to illustrate the effect of Cu content in solder on the formation of $(Cu_{1-y},Ni_y)_6Sn_5$ IMC near the chip side, as shown in Fig. 9. The mechanism of interfacial reaction and compound formation in the Sn-3.0Ag-0.5Cu joints during assembly and aging was established and is plotted schematically in Fig. 10 with the aid of the interfacial microstructure, IMC growth behavior, and Sn-Ag-Cu ternary diagram.

- The saturation solubility of Cu in the molten solder with 3.0 wt.% Ag at 240°C is about 1.51 wt.%, which is larger than the Cu content in the molten solder for Sn-3.0Ag-0.5Cu joint. Therefore, the molten solder in the Sn-3.0Ag-0.5Cu joint was able to dissolve the Cu layer completely during assembly, as shown in the schematic diagram (Fig. 10a).
- The Ni(V) layer was then exposed to be in contact with the molten solder (Fig. 10b), and thus Ni in Ni(V) layer dissolved into the molten solder.
- After the concentration of (Cu + Ni) in the molten solder reached the saturated solubility, the Ni(V) layer reacted with the molten solder to form rod-like $(Cu_{1-y},Ni_y)_6Sn_5$ IMC with higher Ni content, as exhibited in Fig. 10c. The morphology of $(Cu_{1-y},Ni_y)_6Sn_5$ IMC in the as-assembled Sn-3.0Ag-0.5Cu joints was rod-like (Fig. 5a), and Ni atoms in the Ni(V) layer thus easily migrated through the grain boundary of $(Cu_{1-y},Ni_y)_6Sn_5$ IMC. The consumption rate of Ni(V) layer adjacent to the grain boundary of $(Cu_{1-y},Ni_y)_6Sn_5$ should be faster. Therefore, the Ni(V) layer adjacent to grain boundary of $(Cu_{1-y},Ni_y)_6Sn_5$ was consumed and then replaced by Sn patches during assembly (Figs. 2a and 10c).
- As mentioned before, the $(Cu_{1-y},Ni_y)_6Sn_5$ IMC in the Sn-3.0Ag-0.5Cu joints grew with a rate constant of 4.63×10^{-8} cm/sec$^{0.5}$ during 500 h aging at 150°C (Figs. 8 and 10d).
- If the aging time was more than 500 h, the $(Cu_{1-y},Ni_y)_6Sn_5$ IMC dissolved with the rate constant of 2.60×10^{-8} cm/sec$^{0.5}$ (Figs. 8 and 10e). On the other hand, the Sn patches gradually grew with aging time, as shown in Figs. 2 and 10c–10e.

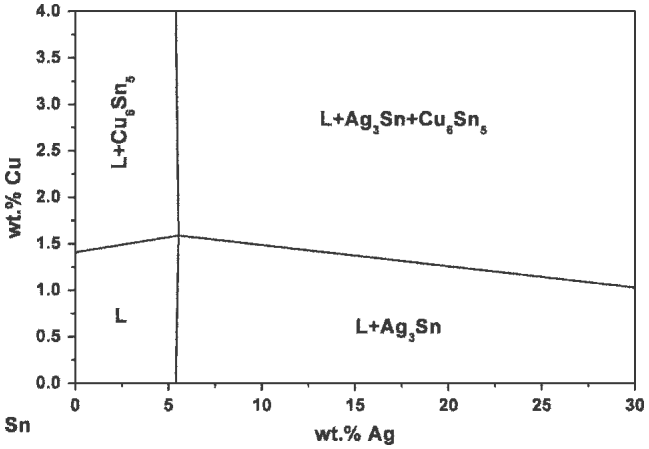

Fig. 9. Enlarged Sn corner of the Sn-Ag-Cu ternary isotherm at 240°C.[5,26–30]

On the other hand, the interfacial reaction mechanism for the Sn-3.0Ag-1.5Cu joint during assembly and aging was also proposed and is shown in Fig. 11.

- If the Cu layer completely dissolved into molten solder during assembly, the Cu content in the solder was 1.71 wt.%, which was greater than the saturation limit at 240°C. Therefore, only portions of Cu layer dissolved into molten solder (Fig. 11a).
- The Sn-Ag-Cu ternary isotherm in Fig. 9 indicates that the maximum weight percent of dissolved Cu in the solder was 1.51 wt.% in the Sn-3.0Ag solder at 240°C. From Eq. (2), the maximum weight of Cu layer dissolved into solder was measured and equaled to be 1.97×10^{-8} g for the Sn-3.0Ag-1.5Cu joint. However, the 0.28 μm Cu layer was dissolved into molten solder, and the Cu content in the molten solder should reach the saturation limit. Therefore, the thickness of remained Cu layer in UBM was 0.22 μm, as displayed in Fig. 11b.

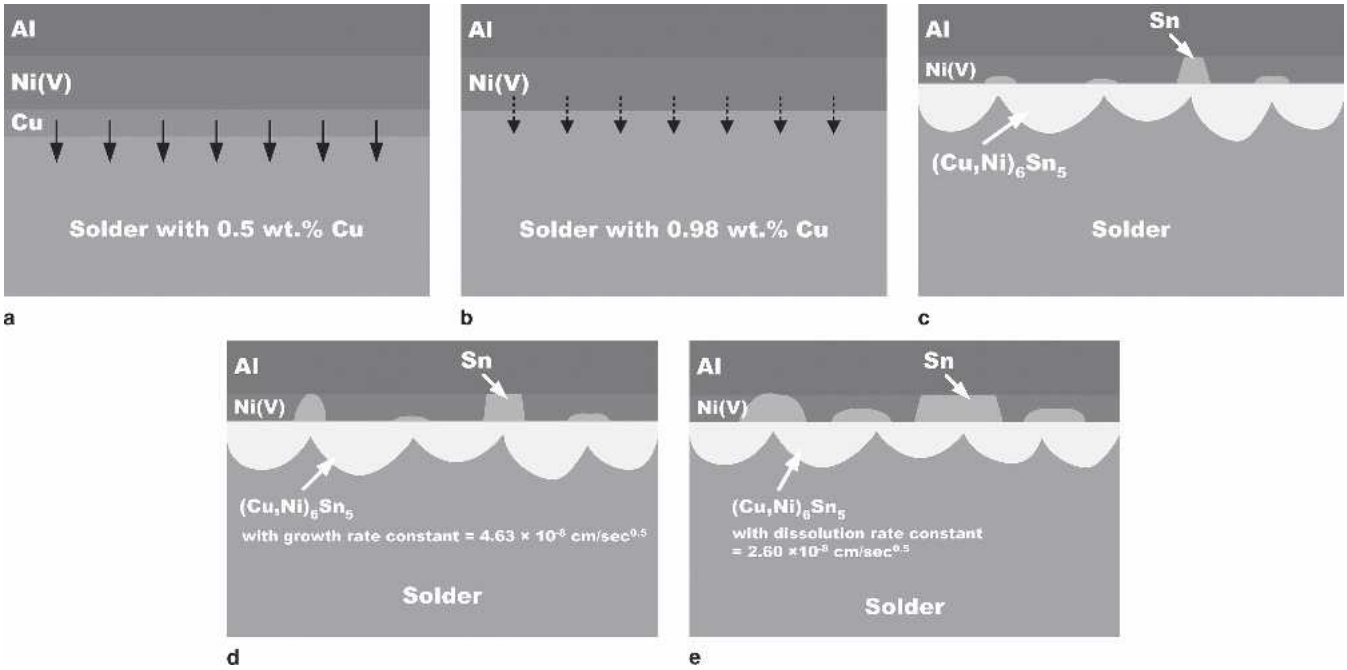

Fig. 10. Schematic diagram showing the proposed interfacial reaction mechanism in the Sn-3.0Ag-0.5Cu joints with Al/Ni(V)/Cu UBM during (a–c) assembly process and (d, e) aging at 150°C.

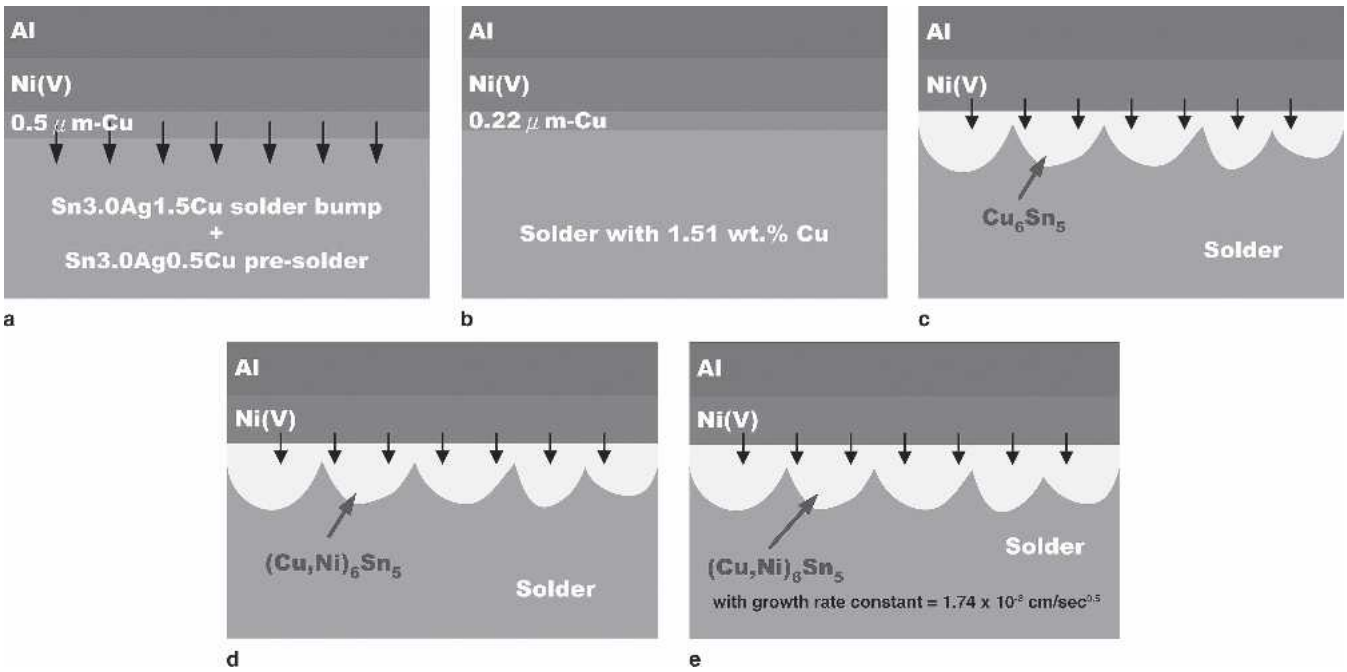

Fig. 11. Schematic diagram showing the proposed interfacial reaction mechanism in the Sn-3.0Ag-1.5Cu joints with Al/Ni(V)/Cu UBM during (a–d) assembly process and (e) aging at 150°C.

- After the Cu content in the molten solder reached the saturation limit, the remaining Cu layer would react with solders to form the nodular-type Cu_6Sn_5 IMC adjacent to the Ni(V) layer (Fig. 11c).
- Because the Ni(V) layer is not exposed to the liquid phase of the Sn-3.0Ag-1.5Cu solder, Ni was incorporated into the Cu_6Sn_5 IMC through slow solid-state diffusion to form $(Cu_{1-y},Ni_y)_6Sn_5$ IMC (Fig. 11d). Most of the Ni(V) layer was thus preserved during assembly process.
- During aging at 150°C up to 2,000 h, the $(Cu_{1-y},Ni_y)_6Sn_5$ IMC gradually grew with aging time, and the rate constant was 1.74×10^{-8} cm/sec$^{0.5}$. In contrast, the Ni(V) layer of Al/Ni(V)/Cu UBM was preserved even after 2,000 h aging, as shown in Figs. 6 and 11e.

From cross-sectional images, the average thickness of unreacted Ni(V) layer after assembly was 0.22 μm for Sn-3.0Ag-0.5Cu joint and 0.50 μm for Sn-3.0Ag-1.5Cu joint, respectively. Thus, the consumption rate of Ni(V) layer for the Sn-3.0Ag-0.5Cu joints was 1.56 times for the Sn-3.0Ag-1.5Cu joints during assembly. In fact, the mechanism of $(Cu_{1-y},Ni_y)_6Sn_5$ IMC formation in Sn-3.0Ag-0.5Cu was different from that in the Sn-3.0Ag-1.5Cu joints. Thus, the amount of Ni dissolved in $(Cu_{1-y},Ni_y)_6Sn_5$ IMC for Sn-3.0Ag-1.5Cu joint was less than that for Sn-3.0Ag-0.5Cu joint, as exhibited in Table I.

CONCLUSIONS

In the Sn-3.0Ag-0.5Cu joints, the Cu layer in the Al/Ni(V)/Cu UBM was completely dissolved into the molten solder during assembly process. The Ni(V) layer was exposed and thus in contact with the molten solder, resulting in the formation of rod-like $(Cu_{1-y},Ni_y)_6Sn_5$ IMC. During aging at 150°C, the Ni(V) layer was gradually consumed and replaced by Sn patches. For aging up to 2,000 h, the area ratio of Sn patches to [Ni(V) layer + Sn patches] increased to 61.6%. On the other hand, $(Cu_{1-y},Ni_y)_6Sn_5$ IMC gradually grew with aging time before 500 h aging. Due to supply limitation of the Ni(V) layer, the $(Cu_{1-y},Ni_y)_6Sn_5$ was dissolved after more than 500 h aging and the rate constant was 2.60×10^{-8} cm/sec$^{0.5}$.

For Sn-3.0Ag-1.5Cu joints, the 0.28 μm-Cu layer was dissolved into molten solder during assembly, and the Cu content in the molten solder should reach the saturation limit. The remained Cu layer rapidly reacted with solders to form the nodular-type Cu_6Sn_5, which completely covered the Ni(V) layer. The Ni from Ni(V) layer was thus incorporated into the Cu_6Sn_5 IMC through slow solid-state diffusion. As a result, the Ni content in $(Cu_{1-y},Ni_y)_6Sn_5$ IMC for Sn-3.0Ag-1.5Cu joint was thus less than that for Sn-3.0Ag-0.5Cu joint. During 2,000 h aging, the growth behavior of $(Cu_{1-y},Ni_y)_6Sn_5$ IMC in the Sn-3.0Ag-1.5Cu joints followed the parabolic rate law. In addition, the Ni(V) layer in the Al/Ni(V)/Cu UBM remained even after 2,000 h aging.

ACKNOWLEDGEMENTS

The financial support and joint assemblies preparation from Taiwan Semiconductor Manufacturing Company (TSMC) are acknowledged. Partial financial assistance from the Ministry of Economic Affairs, Taiwan, under Contract No. 94-EC-17-A-08-S1-0003 is also appreciated.

REFERENCES

1. L.F. Miller, *IBM Journal of Research and Development* 13, 239 (1969).
2. J.H. Lau, *Flip Chip Technologies* (New York: McGraw-Hill, 1996), pp. 26–30.
3. G.R. Blackwell, *The Electronic Packaging Handbook* (Boca Raton, FL: CRC Press, 2000), pp. 4.4–4.25.
4. D.R. Frear and S. Thomas, *MRS Bull.* 28, 68 (2003).
5. M. Li, F. Zhang, W.T. Chen, K. Zeng, K.N. Tu, H. Balkan, and P. Elenius, *J. Mater. Res.* 17, 1612 (2002).
6. F. Zhang, M. Li, C.C. Chum, and K.N. Tu, *J. Mater. Res.* 17, 2757 (2002).
7. F. Zhang, M. Li, C.C. Chum, and Z.C. Shao, *J. Electron. Mater.* 32, 123 (2003).
8. F. Zhang, M. Li, B. Balakrisnan, and W.T. Chen, *J. Electron. Mater.* 31, 1256 (2002).
9. G.Y. Jang, J.G. Duh, H. Takahashi, S.W. Lu, and J.C. Chen, *J. Electron. Mater.* 35, 1745 (2006).
10. J.S. Ha, T.S. Oh, and K.N. Tu, *J. Mater. Res.* 18, 2109 (2003).
11. J.I. Goldstein, D.E. Newbury, D.C. Joy, C.E. Lyman, P. Echlin, E. Lifshin, L. Sawyer, and J.R. Michael, *Scanning Electron Microscopy and X-ray Microanalysis* (New York: Plenum, 2003), pp. 391–420.
12. G.Y. Jang, C.S. Huang, L.Y. Hsiao, J.G. Duh, and H. Takahashi, *J. Electron. Mater.* 33, 1118 (2004).
13. G.Y. Jang and J.G. Duh, *J. Electron. Mater.* 34, 677 (2005).
14. R.E. Reed-Hill and R. Abbaschian, *Physical Metallurgy Principles* (Boston, MA: PWS Publishing Company, 1994), pp. 272–299.
15. W.D. Callister, *Materials Science and Engineering: An Introduction* (New York: John Wiley & Sons, 1997), pp. 8–27.
16. E. Philofsky, *Solid-State Electron.* 13, 1391 (1970).
17. G.V. Kidson, *J. Nucl. Mater.* 3, 21 (1961).
18. G.Y. Jang, J.G. Duh, H. Takahashi, and D. Su, *J. Electron. Mater.* 35, 323 (2006).
19. S. Choi, J.P. Lucas, K.N. Subramanian, and T.R. Bieler, *Journal of Materials Science: Materials in Electronics* 11, 497 (2000).
20. D.Q. Yu, C.M.L. Wu, C.M.T. Law, L. Wang, and J.K.L. Lai, *J. Alloys Compd.* 392, 192 (2005).
21. M.J. Rizvi, Y.C. Chan, C. Bailey, H. Lu, and M.N. Islam, *J. Alloys Compd.* 407, 208 (2006).
22. K.N. Tu, J.W. Mayer, and L.C. Feldman, *Electronic Thin Film Science for Electrical Engineers and Materials Scientists* (New York: Macmillan, 1992), pp. 302–333.
23. N. Noolu, N. Murdeshwar, K. Ely, J. Lippold, and W. Baeslack III, *Metall. Mater. Trans. A* 35, 1273 (2004).
24. N. Noolu, N. Murdeshwar, K. Ely, J. Lippold, and W. Baeslack III, *J. Mater. Res.* 19, 1374 (2004).
25. K.N. Tu and K. Zeng, *Mater. Sci. Eng. R* 34, 1 (2001).
26. H. Ohtani, K. Okuda, and K. Ishida, *J. Phase Equilib.* 16, 416 (1995).
27. J.H. Shim, C.S. Oh, B.J. Lee, and D.N. Lee, *Z. Metallkd.* 87, 205 (1996).
28. F.H. Hayes, H.L. Lukas, G. Effenberg, and G. Petzow, *Z. Metallkd.* 77, 749 (1986).
29. C.S. Oh, J.H. Shim, B.J. Lee, and D.N. Lee, *J. Alloys Compd.* 238, 155 (1996).
30. K.W. Moon, W.J. Boettinger, U.R. Kattner, F.S. Biancaniello, and C.A. Handwerker, *J. Electron. Mater.* 29, 1122 (2000).